Available online at www.sciencedirect.com
ScienceDirect
Catalysis Today 126 (2007) 119–126
CATALYSIS TODAY
www.elsevier.com/locate/cattod

Application of microfabricated reactors for *operando* Raman studies of catalytic oxidation of methanol to formaldehyde on silver

Enhong Cao [a,b], Steve Firth [b,c], Paul F. McMillan [b,c,d], Asterios Gavriilidis [a,b,*]

[a] *Department of Chemical Engineering, University College London, Torrington Place, London WC1E 7JE, UK*
[b] *Materials Chemistry Centre, University College London, Gordon Street, London WC1H 0AJ, UK*
[c] *Department of Chemistry, Christopher Ingold Laboratory, University College London, 20 Gordon Street, London WC1H 0AJ, UK*
[d] *Davy-Faraday Research Laboratory, Royal Institution of Great Britain, 21 Albemarle Street, London W1X 4BS, UK*

Available online 14 December 2006

Abstract

Operando Raman-GC studies of the catalytic oxidation of methanol to formaldehyde on silver using a microfabricated reactor as a reactor cell are presented. The microreactor is made of silicon and glass with a wide reaction channel of 8 mm and a channel depth of 120 μm. The silver catalyst is incorporated into the microchannel by sputter coating. The reaction is performed at atmospheric pressure, temperature between 723 and 813 K with a feed containing 8.75% CH_3OH, 3.5% O_2 and 6.63% H_2O (He as balance) at residence time of 6–7 ms at reaction temperature. Raman spectra of the silver catalyst after exposure to 4.1% O_2 (He as balance) at 773 K show the presence of subsurface (at 640 cm^{-1}) and surface (at 810 cm^{-1}) atomic oxygen species. During an activation procedure consisting of repeated oxidation/reaction cycles at 773 K, the 810 cm^{-1} band disappears immediately after introducing a $CH_3OH/O_2/H_2O$/He mixture, indicating that this surface atomic oxygen species participates in the reaction. The 810 cm^{-1} band is not observed in the subsequent oxidation/reaction cycles; instead a broad feature between 400 and 800 cm^{-1} appears which may be associated with a severe restructuring of the catalyst by methanol oxidation. The catalyst stabilizes after three oxidation/reaction cycles as shown by improved and approximately constant CH_2O selectivities. This is accompanied by Raman spectra with sharp definition of the 400–800 cm^{-1} band, indicating the importance of stabilization of subsurface oxygen species in obtaining high CH_2O selectivity. Deactivation of the catalyst due to carbon deposition is observed when a feed without H_2O is introduced into the reactor, as demonstrated by bands at 1350 and 1585 cm^{-1} in the Raman spectra and by decreased conversion of CH_3OH with reaction time. The work presented demonstrates that microfabricated reactors can be easily integrated with Raman spectroscopy and GC for *operando* studies.
© 2006 Elsevier B.V. All rights reserved.

Keywords: *In situ* Raman; Microreactor; Operando; Catalytic oxidation; Silver; Methanol; Formaldehyde

1. Introduction

Raman spectroscopy has become a popular catalyst characterization method, particularly for *in situ* applications in selective catalytic oxidations even under extreme pressures and high temperatures [1,2]. By incorporating an analytical instrument, such as GC and MS, the methodology of *operando* spectroscopy, permits the detection and analysis of chemisorbed species and possible catalytic intermediates which are related to simultaneous changes of the catalytic activity under reaction conditions [3–6]. For *operando* Raman studies, the experiments for catalyst testing and spectroscopic measurement have to be combined, and the design of the *in situ* Raman cell is of crucial importance for simultaneously obtaining catalytic and spectroscopic results. Several *in situ* Raman cells have been reported [2,7–9]. These cells were designed with rotating sample holders or rotating laser beams to minimise local heating effects [7,8], or with reactive gases flowing through a loose powder to mimic a typical plug flow [9]. However, most of the arrangements of the cells do not result in plug-flow conditions, and mass and temperature gradients may be present in the cells or in the catalyst samples due to large cell volume, pressed sample wafers or large optical windows [2,6].

The development of microfabricated reactors for the study of heterogeneous catalytic reactions may offer an opportunity to

* Corresponding author at: Department of Chemical Engineering, University College London, Torrington Place, London WC1E 7JE, UK.
Tel.: +44 20 76793811.
E-mail address: a.gavriilidis@ucl.ac.uk (A. Gavriilidis).

0920-5861/$ – see front matter © 2006 Elsevier B.V. All rights reserved.
doi:10.1016/j.cattod.2006.11.002

surpass the obstacles mentioned above and improve the performance of *in situ* Raman cells. The advantages of microfabricated reactors, such as enhanced heat and mass transfer and precise control of reaction temperature are derived from their reduced scale (reaction channels with features of a few microns to hundreds of microns) [10,11]. Microreactors fabricated on silicon have been successfully used for catalytic oxidative dehydrogenation of methanol [12]. The results showed the benefits of using microreactors in the study of highly exothermic reactions. Isothermal reaction conditions can be easily achieved due to the high surface to volume ratio and a small amount of reaction mixture involved. This, along with the capability of varying reactant concentration safely over a wide range, makes it possible to use microfabricated reactors as powerful tools for kinetic studies. In this paper, we demonstrate the application of a microfabricated reactor in *operando* Raman-GC studies for the catalytic oxidation of methanol to formaldehyde on silver.

Due to the importance of formaldehyde in the organic synthetic industry, significant research efforts have focused on understanding the catalytic behaviour of silver and the reaction mechanism. The surface properties of silver and the interaction between oxygen and silver surface have been investigated intensively. Most information has come from UHV studies with low exposure to molecular oxygen and methanol [13–20], but the application of *in situ* Raman spectroscopy has allowed the study of interactions between oxygen and silver under practical conditions [21–33]. These studies used Raman spectroscopy for *in situ* investigation under reaction conditions but without determining quantitatively catalyst activity. Recently Waterhouse et al. [34] studied the reaction on an electrolytic silver catalyst using *in situ* Raman spectroscopy, X-ray photoelectron spectroscopy (XPS) and SEM as well as a fixed-bed microreactor. The *in situ* Raman studies were carried out under conditions close to those employed industrially. The catalytic studies were however carried out separately. In this work we investigate the reaction by simultaneously performing both *in situ* Raman and on-line catalyst activity measurements in the same catalyst system.

2. Experimental

The microfabricated reactor (see Fig. 1), which was used as an *in situ* reactor cell, was made of silicon and glass and was fabricated by photolithography and anodic bonding [12]. Silver catalyst can be incorporated into the microreaction channel by thin film technology before anodic bonding or by packing silver particles into the reactor after bonding. In this paper, sputter-coated silver was used as catalyst. The coating was carried out at room temperature under argon at a current of 150 mA using a Turbo Sputter Coater (K675XD, Emitech). A shadow mask was used to confine the silver coated within the reaction area of the reactor. The microfabricated reactor had a wide reaction channel of 8 mm and a channel depth of 120 μm. The length of the silver coated area was 12.5 mm and the thickness of the silver layer was 0.25 μm achieved by three continuous coating cycles. Each cycle was 155 s giving a silver thickness of 83 nm.

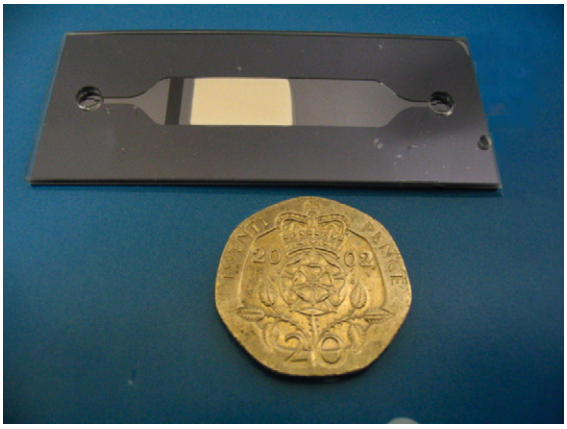

Fig. 1. Silicon-glass microreactor. Overall size: 25 mm × 63 mm.

The silicon reactor was covered by 1 mm thick glass piece (Corning 7740) with inlet and outlet holes, through anodic bonding. Before bonding, the silver-coated microreactor was calcined at 873 K in an oven in air for 2 h. Anodic bonding was then carried out using a home-made bonder at 723 K and 1 kV in air. After bonding, the microreactor was mounted onto a heating block where a clamp with structures for Swagelok nuts and graphite ferrules was used to seal the inlet/outlet tubings. The whole assembly was insulated using structured ceramic boards with a small window for access of the laser. The reaction temperature could be controlled up to 823 K and the maximum temperature difference over the reaction zone was 2 K [12].

In the *operando* Raman-GC study, the microreactor assembly was placed vertically at the side of the microscope and was connected to a gas control manifold system and a microevaporator/mixer, so that oxygen or methanol containing reaction gas mixtures could be introduced, as shown schematically in Fig. 2. The outlet from the microreactor was directed to a GC (ThermoQuest, Trace) which was equipped with a Carboxen 1006 column. CO/O_2, CO_2, H_2O, CH_2O and CH_3OH were separated and detected using a TCD. The tubing between the microevaporator and the GC was heated and insulated to keep it at 373 K in order to prevent any possible condensation of the reaction mixture. The conversion of CH_3OH and yield of products were calculated as follows:

$$\text{conversion}\,(\%) = \frac{\text{mol(MeOH, in)} - \text{mol(MeOH, out)}}{\text{mol(MeOH, in)}} \times 100$$

$$\text{yield}\,(\%) = \frac{\text{mol(product)}}{\text{mol(MeOH, in)}} \times 100$$

Raman spectra were obtained using a Renishaw inVia Raman spectrometer coupled to a Leica microscope. Spectra were excited using the 514.5 nm line from a LaserPhysics argon ion laser. A 90° arm was fixed to the microscope to direct the laser beam to the microreactor assembly. This arm was fitted with a Mitutoyo 50× SLWD objective with a working distance of 21 mm, to give a laser power at the microreactor of ca. 3 mW. Raman scattered light was detected with a CCD. Spectra were recorded with an integration time of 20 s and averaged three times.

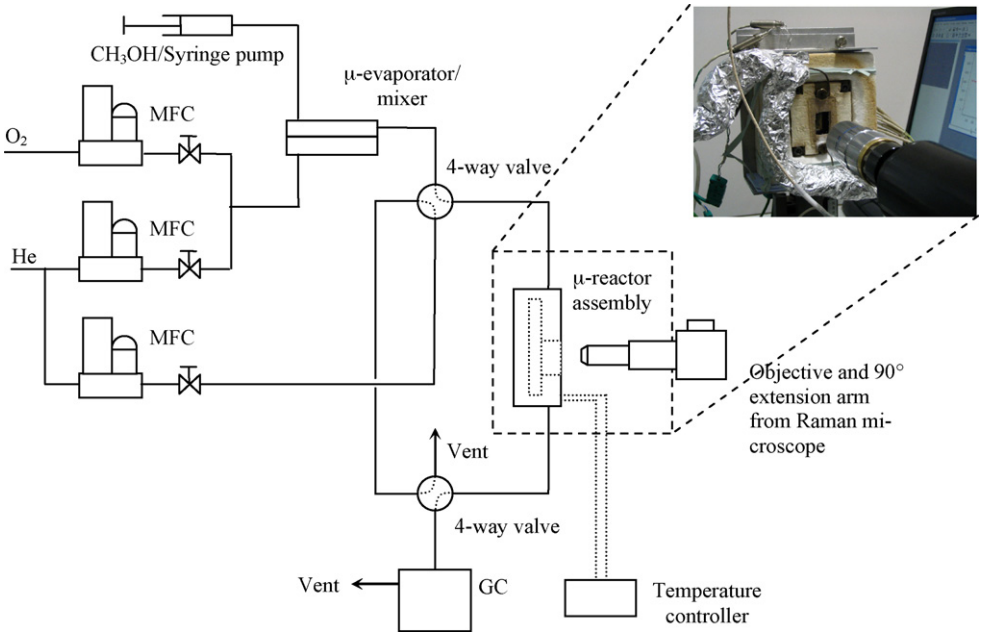

Fig. 2. Schematic of the experimental setup for the *operando* Raman-GC study.

In a typical experiment, pretreatment of the catalyst was carried out at 523 K and then at 673 K, for 1 h at each temperature, with a flow of helium to remove adsorbed surface species and impurities. The silver surface was then treated by a flow of O_2/He mixture at 673 K for 1 h and at 773 K for 2 h. The reactor was cooled down to 523 K and a continuous flow of O_2/He or $O_2/CH_3OH/H_2O$/He was introduced to provide the desired environment and the reactor temperature was varied from 523 to 823 K. Raman spectra were recorded from the surface of the silver catalyst at each desired temperature while the outlet reaction mixture was also sampled and analysed by the GC. The typical composition for O_2/He mixture was 4.1% O_2 with He as balance and the $O_2/CH_3OH/H_2O$/He mixture contained 8.75% CH_3OH, 3.5% O_2 and 6.63% H_2O with He as balance. The residence time at reaction temperature was 6–7 ms in all experiments.

3. Results and discussion

3.1. SEM characterization of the silver catalyst

The surface morphology of the prepared silver catalyst was examined by SEM. Fig. 3 shows the sputter-coated silver before and after treatment in air at 873 K. It has been reported that sputter-coated silver on silicon wafer shows fine columnar structures, epitaxial films or islands depending on sputtering conditions [35,36]. Fig. 3(a) shows that the sputter-coated silver exhibits a relatively smooth surface structure with fine, densely packed particles. After calcination in air at 873 K, particles conglomerate into large islands and the thin film is re-crystallized (Fig. 3(b)). Similar observations have been made for silver films deposited on glassy materials where reorganisation of silver occurred by surface diffusion which was enhanced by the presence of O_2 [37]. This silver reorganisation was

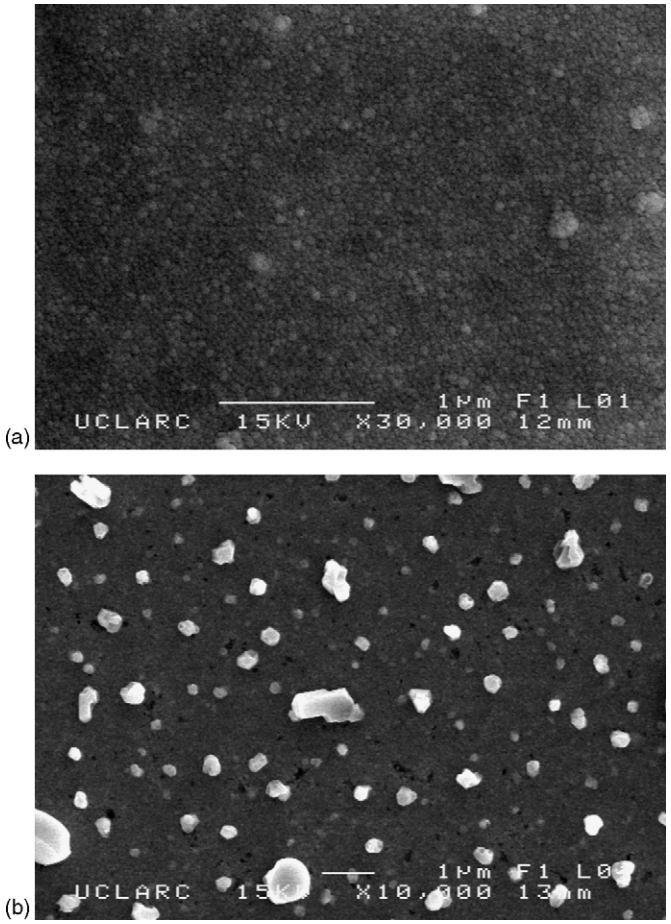

Fig. 3. SEM micrographs of (a) sputter-coated silver and (b) calcined in air at 873 K for 2 h.

observed to occur in four stages: (1) an induction time, during which no holes appear in the film, but hillocks grew on the top surface of films; (2) growth of holes to form a network structure; (3) separation of agglomerates; (4) withdrawal of islands to final, approximately hemispherical, shapes [37]. Fig. 3(b) seems to correspond to stage 4 above.

3.2. Raman spectra of silver surface after bonding and after pretreatment

The silver catalyst was prepared in air and heated during the fabrication process. Hence, some surface oxygen species could have formed and carbon-containing impurities could also have adsorbed on the silver surface. The purpose of the silver surface pretreatment was to remove these species and impurities and to treat the surface under defined conditions. The Raman spectrum recorded at room temperature for the silver after bonding is presented in Fig. 4(a). The spectrum is dominated by sharp peaks at 810 and 780 cm^{-1} due to oxygenated species, that also give rise to broad, weak bands at 350, 570 and 640 cm^{-1} [25,26,29–34]. There is also a weak band at 1585 cm^{-1} that is due to relatively well-ordered graphitic material [38,39]. The spectra of Fig. 4(b) and (c) were obtained at 523 and 673 K with a flow of He through the reactor. At 523 K, the graphite band grew in intensity and broadened, and a broad additional band grew at 1350 cm^{-1}. This indicates the further formation and aggregation of disordered graphitic carbon species [39,40]. It is probable that the carbonaceous material is derived from pyrolysis of hydrocarbon species initially present on the catalyst surface or oil or grease contained in the He carrier gas. By exposure of the silver surface to a flow of O_2/He at 673–773 K, the surface carbon species were completely removed (Fig. 4(d) and (e)).

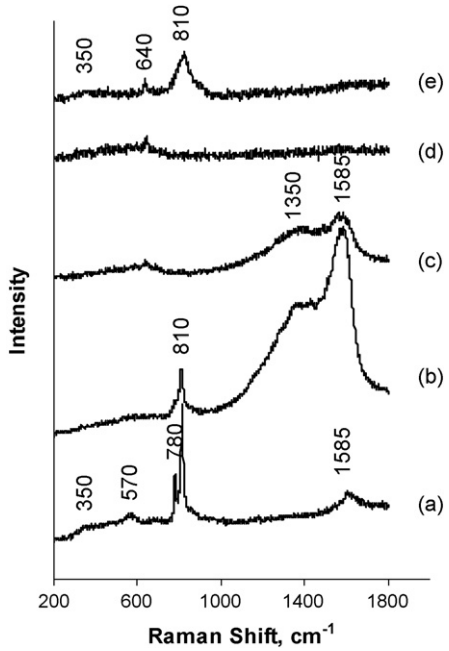

Fig. 4. Raman spectra during silver surface pre-treatment: (a) as-prepared silver catalyst; (b) in He at 523 K; (c) in He at 673 K; (d) in O_2/He at 673 K; (e) in O_2/He at 773 K (O_2 4.1%, He as balance).

The vibrational modes in the 300–1000 cm^{-1} region have been assigned to various oxygenated or hydroxylated species associated with the silver surface. Bao et al. [25] noted that the interaction of H_2O or H_2 with an oxygenated Ag(1 1 1) surface resulted in the creation of subsurface hydroxyl species with a Raman band at 575 cm^{-1}. Millar et al. [30,31] suggested that subsurface hydroxyl species at polycrystalline silver were represented by a band at 570 cm^{-1}, which was observed in Fig. 4(a) for the as-prepared silver catalyst. However, studies with H_2O and D_2O by Wang et al. [32] have cast doubt on the assignment of any bands to hydroxyl species although they did not report any Raman spectra below 600 cm^{-1}. Bands at 600–700 cm^{-1} are indicative of subsurface/bulk atomic oxygen species, denoted O_β, dissolved in the silver lattice [26,29,33,34]. Peaks near 800 cm^{-1} are assigned to the Ag–O–Ag stretching mode of strongly chemisorbed surface atomic oxygen species, O_γ [32]; the band at 350 cm^{-1} is likely due to a bending mode of that species [26,33,34]. O_γ is formed by segregation of O_β from silver bulk to the surface and by the dissociative chemisorption of O_2 on defects when the catalyst is heated in an O_2 atmosphere. It desorbs at temperatures above 573 K but it can exist at temperatures in excess of 923K in the presence of O_2 [34]. The splitting of the O_γ mode into two components at 780 and 810 cm^{-1} could be due to the presence of subsurface oxygen species [29]. A peak at 960 cm^{-1} has been observed in previous studies and assigned to surface atomic oxygen with a Ag=O double bond [32]. This feature was not observed in our studies, possibly due to the high temperatures employed.

The nature and proportion of the oxygen species formed on silver and their Raman spectroscopic signature depends on the exact morphology of the catalyst and can provide some indication of surface reconstruction. Bao et al. [24] observed Raman bands for atomic oxygen species at 631 and 802 cm^{-1}, whose relative intensities depended on Ag-surface orientation. The latter could be altered by pronounced refaceting induced during long exposure to oxygen, as observed by various microscopy and diffraction techniques [16]. Millar et al. [29] reported that subsurface oxygen species (at 640 cm^{-1}) were only detected on a highly defective silver sample, while Bao et al. [17] observed these species on silver single crystals after considerable surface reconstruction had occurred. Waterhouse et al. reported that the 640 cm^{-1} band associated with O_β species was only prominent in the spectra taken from catalysts possessing a high proportion of surface grain boundaries [34]. In our study, evidence that surface reconstruction occurred following calcination is provided by the observed morphology in Fig. 3.

Heating the silver catalyst to 523–673 K in a flow of He led to a reduction in the intensity of bands associated with oxygenated species due to desorption from the surface, initially accompanied by an increase followed by a decrease in the signal due to disordered carbonaceous material (Fig. 4(b) and (c)). By 673 K, the 640 cm^{-1} band due to subsurface atomic oxygen species (O_β) was visible in the spectra, along with a weak broad background signal in the 200–700 cm^{-1} region. This could indicate the migration of O_γ to O_β sites in this

temperature range (Fig. 4(c)). At 673 K an O_2/He flow was introduced into the reactor for 1 hr (Fig. 4(d)) and then the reactor temperature was increased to 773 K for 2 h (Fig. 4(e)). With the introduction of the O_2/He mixture the carbonaceous species were completely removed at 673 K (Fig. 4(d)). The 640 cm^{-1} peak remained present and became better defined in the spectra after raising the temperature to 773 K in a flow of O_2/He (Fig. 4(d) and (e)), while the broad low-frequency background disappeared, allowing the weak broad feature at 350 cm^{-1} to be observed (Fig. 4(e)). At 773 K in the O_2/He mixture, a broadened feature due to chemisorbed surface Ag–O–Ag (O_γ) species reappeared at 810 cm^{-1} (Fig. 4(e)).

3.3. Silver catalyst during activation by oxidation/reaction cycles

An activation procedure was applied, consisting of repeated cycles of oxidation in O_2/He (60 min) and reaction in CH_3OH/O_2/H_2O/He mixtures (90 min) at 773 K [12]. The compositions of the reaction gas mixtures were described previously. The surface composition of the silver catalyst and the composition of the gas mixture at the reactor outlet were monitored during the activation. The results are shown in Fig. 5.

The first activation cycle started with the treated silver catalyst described above (Fig. 5(a)). Immediately upon introducing the reaction mixture, the O_γ Raman band at 810 cm^{-1} as well as the weaker broad feature at 350 cm^{-1} disappeared, and were replaced by a broad asymmetric feature between 400 and 800 cm^{-1} with a maximum near 690 cm^{-1} (Fig. 5(b)). This broad feature is obviously composed of at least two components. Spectra recorded at intermediate times between Fig. 5(a) and (b) are shown in Fig. 6. The spectrum at 5 min after introducing the reaction mixture contained only a broad asymmetric feature in the region of 200–800 cm^{-1}

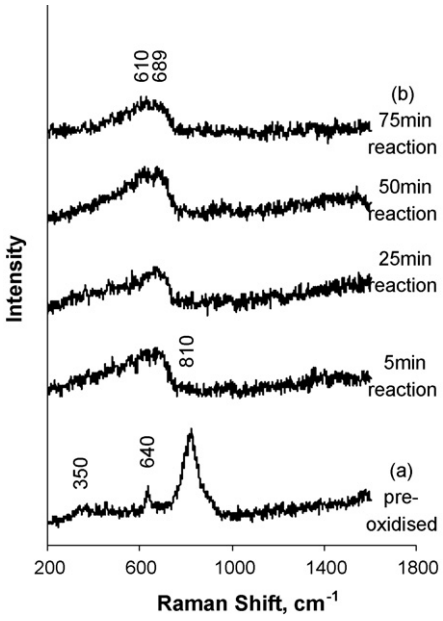

Fig. 6. Raman spectra during the first reaction cycle of the activation procedure of Fig. 5.

(Fig. 6). During the 75 min reaction period, this feature changed slightly in shape while the low-frequency background disappeared leaving a broad asymmetric feature between 400 and 800 cm^{-1} with a maximum near 600–690 cm^{-1} at the end of first reaction step. Fig. 6(b) is the same as Fig. 5(b).

In the second oxidation step, the silver surface was exposed to the O_2/He flow again for 1 h. The bands at 810 and 350 cm^{-1} did not reappear, instead the broad asymmetric feature between 400 and 800 cm^{-1} extended to lower frequency and a prominent maximum appeared at 689 cm^{-1} (Fig. 5(c)). On switching to the reaction mixture and allowing the reaction to

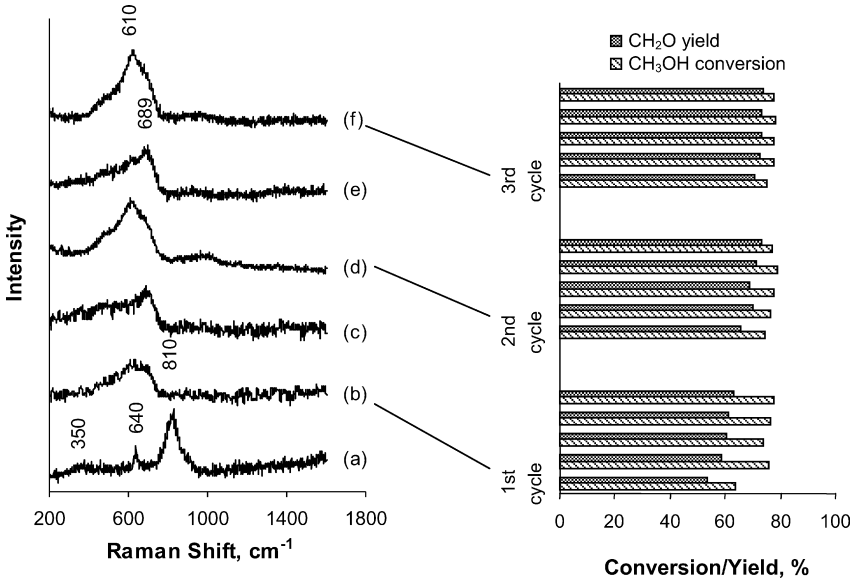

Fig. 5. *Operando* Raman-GC results of the silver catalyst during the activation cycles at 773 K. Raman spectra at the end of: (a) oxidation; (b) reaction; (c) oxidation; (d) reaction; (e) oxidation; (f) reaction steps. Five samples were analysed by GC at 14 min intervals in each reaction step. Oxidation in a flow of O_2 (4.1%), He as balance; reaction in a flow of CH_3OH (8.75%), O_2 (3.5%) and H_2O (6.63%), He as balance.

take place, the spectrum of Fig. 5(d) showed a shift of the maxima from 689 to 610 cm^{-1}, resulting in a broad complex band between 400 and 800 cm^{-1}. In the third oxidation step, similar spectra to those observed in the second oxidation step were recorded as the asymmetric band extended to lower frequency again while the maximum shifted from 610 to 689 cm^{-1} (Fig. 5(e)). The spectrum of the silver in the following reaction step, Fig. 5(f), was very similar to that of Fig. 5(d), but with slightly sharper definition. The spectra of Fig. 5(e) and (f) were repeatable with further oxidation-reaction cycles. The activity of the silver catalyst became stable after three oxidation cycles, which was confirmed by monitoring the composition of the product mixture using GC analysis.

GC analysis was carried out at each reaction step. The first sample of the reaction products was taken 15 min after introducing the reaction gas mixture. Subsequent samples were analysed at 14 min intervals and a total of five samples were analysed in each reaction step. The yield/conversion data are plotted in Fig. 5. It can be seen that the reactivity of the silver catalyst remained approximately constant but CH_2O yield (and selectivity) gradually increased with the number of cycles, reaching a stable value after the third oxidation cycle.

The broad feature between 400 and 800 cm^{-1} seen during the reaction cycle and shown in Fig. 5(d) and (f) is similar to that observed by Millar et al. [30] on the surface of silver(I) oxide exposed to a flow of oxygen saturated with methanol at 773 K. Waterhouse et al. [34] also observed a similar broad band between 500 and 700 cm^{-1} on electrolytic silver at 973 K under a flow of CH_3OH/O_2/He mixture. The broad feature between 400 and 800 cm^{-1} is obviously an indication of the concurrent presence of different oxygenated species. Millar et al. has assigned a band at 610 cm^{-1} to subsurface oxygen species whose bonding has been influenced by the presence of neighbouring subsurface hydroxyl groups and a band at 689 cm^{-1} to ν(Ag=O) modes of strongly bound atomic oxygen atoms situated on a silver surface containing a high amount of subsurface hydroxyl groups [30,31]. A band at 575 cm^{-1} has been previously assigned to subsurface hydroxyl species by several researchers [25,30,34,41].

The instant disappearance of the bands at 350 and 810 cm^{-1} on exposure to the reaction mixture (Fig. 6) indicates that the strongly chemisorbed surface atomic oxygen species, O_γ, participated in the reaction. The weakening of the 800 cm^{-1} Raman band on exposure of silver to a methanol oxidation environment was observed by Wang et al. [32] and Waterhouse et al. [34]. They also observed the development of a very broad and weak feature in the ~700–900 cm^{-1} region indicating the co-presence of other oxygen species. A band at 870 cm^{-1} was assigned to the Ag–O–Ag surface species shifting from 800 cm^{-1} by induction of either the reactant CH_3OH or the product H_2O [32,34]. However, this feature is extremely weak and broad in the present study (Fig. 5(d) and (f)). This may be attributed to the highly reactive catalyst and steady-state operation conditions producing a catalyst surface with a very low concentration of this oxygen species. The activity of silver in the microreactor was found to be much higher than that in a laboratory fixed-bed reactor using electrolytic silver in similar studies by Waterhouse et al. [34]. The average reaction rate of CH_3OH based on silver surface area at 810K was calculated as ~10 times higher in the microreactor than that in the fixed-bed reactor [34]. This high reactivity may be due to different catalyst structure and/or the absence of mass transfer resistance in the microfabricated reactor. It is therefore possible that the concentration of the reactive oxygen species, O_γ, might be too low in the current study to be detected.

It is notable that after reaction of CH_3OH on the silver catalyst, re-oxidizing the silver in a 4.1% O_2 flow did not recreate the bands at 350 and 810 cm^{-1} (Fig. 5(c) and (e)) as happened for the freshly prepared silver surface (Fig. 4(e)). This is due to the low O_2 concentration in this atmosphere because we observed that the bands at 350 and 810 cm^{-1} regained their intensity with a 10% O_2 flow through the reactor. Waterhouse et al. [34] re-exposed their silver catalyst into a pure O_2 flow after oxidation of CH_3OH and the bands at 350 and 810 cm^{-1} regained their initial intensity. The fact that the 810 cm^{-1} band is observed during the first oxygen treatment (Fig. 5(a)) but not during the oxidation treatment following reaction cycles (Fig. 5(c) and (e)) may be associated with a severe restructuring of the silver surface by methanol oxidation. Such restructuring and pinhole formation have been observed by various researchers [16,30,34]. The repeatable spectra of Fig. 5(e) and (f) and the constant conversion and yield for CH_3OH and CH_2O demonstrate a stable reaction activity of the silver catalyst. Improved yield of CH_2O accompanied with a sharper definition of the 400–800 cm^{-1} band and of the 610 cm^{-1} peak during activation may indicate the importance of stabilization of subsurface oxygen species in obtaining high CH_2O selectivity.

3.4. Influence of reaction temperature on catalyst composition and performance

The reaction was investigated over a temperature range of 723–813 K in a reaction gas mixture of $CH_3OH/O_2/H_2O$/He as described previously. The Raman spectra along with the corresponding GC analysis results are presented in Fig. 7. The Raman spectra are similar to those of Fig. 5(d) and (f) with a broad feature between 400 and 800 cm^{-1}. The oxygenated species which could be contributing to this broad band have been discussed above. With the increase of reaction temperature, some slight changes of the shoulder at 689 cm^{-1} can be detected, although overall no significant change of the spectra is observed. GC analysis showed that the conversion of CH_3OH increased from 53 to 80% in this temperature range. The yield of CH_2O also increased with the reaction temperature from 43.3 to 73.5% while that of CO_2 decreased slightly, leading to an increased selectivity to CH_2O from 81.8 to 92.1%.

Waterhouse et al. [34] and Bao et al. [26] observed on electrolytic silver catalyst that the bands at 640 cm^{-1} (or 630) and 810 cm^{-1} (or 803) reduced their intensity with increased reaction temperature. Millar et al. [30] observed a broad feature between 400 and 700 cm^{-1} on the surface of silver(I) oxide which was exposed to a flow of oxygen saturated with methanol at 773 K; the characteristic band at 810 cm^{-1}, as observed in

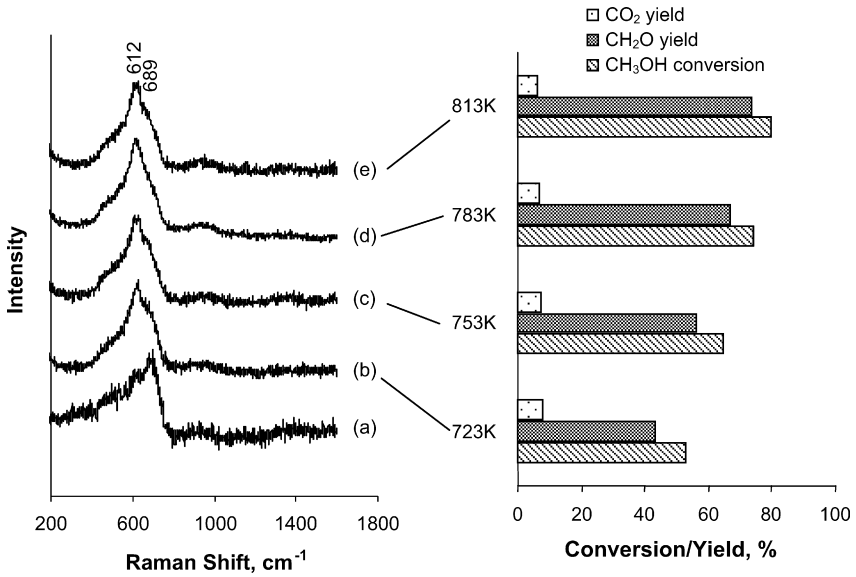

Fig. 7. *Operando* Raman-GC results of the oxidation of CH_3OH to CH_2O: effect of reaction temperature. Raman spectra: (a) oxidation at 723 K; reaction at (b) 723 K; (c) 753 K; (d) 783 K and (e) 813 K. Oxidation in a flow of O_2 (4.1%), He as balance. Reaction in a flow of CH_3OH (8.75%), O_2 (3.5%) and H_2O (6.63%), He as balance.

electrolytic silver catalyst, was not detected. The differences between these two silver samples may be the result of the dependence of oxygen species on catalyst morphology [29]. The behaviour of thin silver film on silicon seems to fall between that of decomposed silver oxide [30] and electrolytic silver [26,34].

3.5. Influence of H_2O in feed on catalyst composition and performance

Fig. 8 shows the results from the *operando* Raman-GC studies of the reaction at 773 K using a reaction gas mixture without H_2O (8.75% CH_3OH, 3.5% O_2 with He as balance). The Raman spectra were quite similar to those observed in Fig. 7 but with the shoulder at 689 cm^{-1} diminished (Fig. 8(a)). Two bands at 1350 and 1585 cm^{-1} grew after the silver catalyst had been in the reaction stream for 30 min (Fig. 8(c)) and were present for the rest of the experiment (Fig. 8(c)–(f)). Meanwhile the GC analysis showed that the conversion of CH_3OH decreased with time from 81 to 62%. The yields of CH_2O and CO_2 also decreased.

The appearance of the bands at 1350 and 1585 cm^{-1} which are attributed to disordered graphitic species, provides evidence that the decrease in CH_3OH conversion using the reaction gas mixture without H_2O is related to the formation of carbonaceous

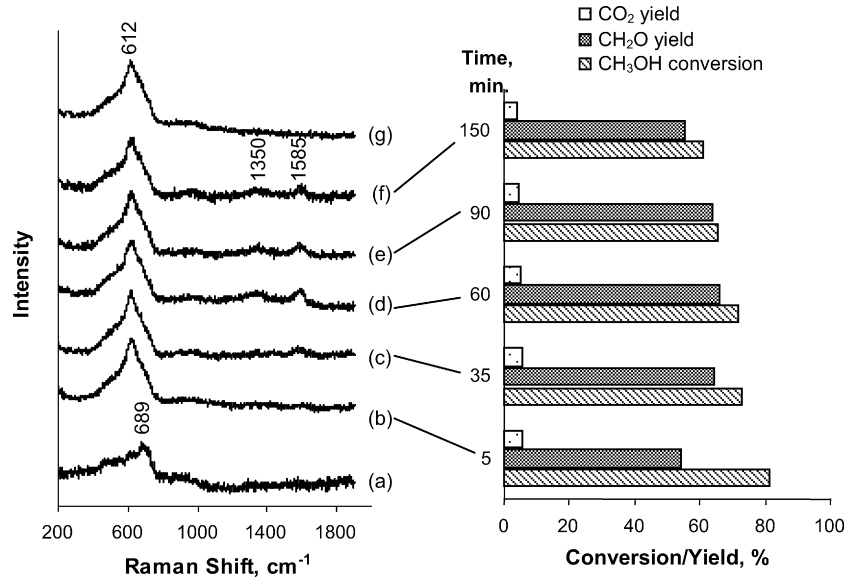

Fig. 8. *Operando* Raman-GC results of the oxidation of CH_3OH to CH_2O: effect of H_2O in feed. Raman spectra: (a) oxidation at 773 K; reaction in H_2O-free feed at (b) 5 min; (c) 35 min; (d) 60 min; (e) 90 min; (f) 150 min and then (g) in a H_2O-containing flow for 5 min. Oxidation in a flow of O_2 (4.1%), He as balance. H_2O-free feed: CH_3OH 8.75%, O_2 3.5%, He as balance. H_2O-containing feed: CH_3OH 8.75%, O_2 3.5% and H_2O 6.63%, He as balance.

deposits on the silver catalyst surface. This was confirmed by re-introducing H_2O into the reaction gas mixture: the 1350 and 1585 cm^{-1} Raman bands disappeared (Fig. 8(g)). Formation of carbonaceous deposits is also consistent with the discrepancy to the carbon balance in the GC analysis at 5 min reaction time. The decrease in CH_3OH conversion in this reaction period is then related to the deactivation of silver by formation of carbonaceous deposits. This coking also explains the observation in previous experiments where the catalyst activity decreased in a H_2O-free reaction gas mixture [12]. In the industrial manufacturing process, H_2O is added into the reaction gas mixture to remove both heat and carbon formed during the reaction.

4. Conclusion

The work presented shows that microfabricated reactors can be easily integrated with *in situ* Raman spectroscopy and simultaneous GC analysis to carry out *operando* studies of catalytic reactions. The silver catalyst, which was sputter-coated inside the microchannel, exhibits island-like particles after being treated in air in 873 K. Raman spectra of the silver catalyst after exposure to 4.1% O_2 (He as balance) at 773 K shows the presence of atomic oxygen species at 640 cm^{-1} (O_β, dissolved in the silver subsurface layers) and 810 cm^{-1} (O_γ, strongly chemisorbed surface atomic oxygen species). During an activation procedure consisting of repeated oxidation/reaction cycles at 773 K, the 810 cm^{-1} band disappears immediately after introducing a $CH_3OH/O_2/H_2O$/He mixture, indicating that O_γ species participates in the reaction. In the subsequent oxidation/reaction cycles, the 810 cm^{-1} band is not observed; instead a broad feature between 400 and 800 cm^{-1} with a maximum Raman shift at 689 cm^{-1} in the oxidation step and 610 cm^{-1} in the reaction step is observed. The bands at 610 and 689 cm^{-1} have been related to subsurface atomic oxygen species and strongly bound atomic oxygen atoms associated with a reconstructured silver surface. The selectivity to CH_2O is improved and stabilized towards the end of the activation procedure. This is accompanied with a sharp definition of the 400–800 cm^{-1} band and of the 610 cm^{-1} peak, indicating the importance of stabilization of subsurface atomic oxygen species in obtaining high CH_2O selectivity. When increasing the reaction temperature from 723 to 813 K, no appreciable change in the Raman spectra is observed, even though both conversion and CH_2O selectivity increase. Deposition of graphitic carbonaceous species is detected when the feed does not contain H_2O, as shown by bands at 1350 and 1585 cm^{-1} in the Raman spectra. This is accompanied by deactivation of the catalyst, demonstrated by decreased conversion of CH_3OH with reaction time.

Acknowledgments

Financial support from EPSRC, UK is gratefully acknowledged. The installation of the Raman microscope system within the Materials Chemistry Centre at UCL was enabled *via* a UK HEFCE SRIF-2 award.

References

[1] H. Knözinger, Catal. Today 32 (1996) 71.
[2] I.E. Wachs, Top. Catal. 8 (1999) 57.
[3] M.O. Guerrero-Perez, M.A. Banares, Chem. Comm. (2002) 1292.
[4] H. Topsoe, J. Catal. 216 (2003) 155.
[5] B.M. Weckhuysen, Phys. Chem. Chem. Phys. 5 (2003) 4351.
[6] M.A. Banares, Catal. Today 100 (2005) 71.
[7] I.E. Wachs, F.D. Hardcastle, S.S. Chan, Spectroscopy 1 (1986) 30.
[8] F. Benabdelouahab, R. Olier, N. Guilhaume, F. Lefebvre, J.C. Volta, J. Catal. 134 (1992) 151.
[9] G. Mestl, M.P. Rosynek, J.H. Lunsford, J. Phys. Chem. B 101 (1997) 9321.
[10] V. Hessel, S. Hardt, H. Löwe, Chemical Micro Process Engineering, Wiley–VCH, Weinheim, 2004.
[11] A. Gavriilidis, P. Angeli, E. Cao, K.K. Yeong, Y.S.S. Wan, Chem. Eng. Res. Des. 80 (2002) 3.
[12] E. Cao, A. Gavriilidis, Catal. Today 110 (2005) 154.
[13] I.E. Wachs, R.J. Madix, Surf. Sci. 76 (1978) 531.
[14] X. Bao, J. Deng, J. Catal. 99 (1986) 391.
[15] X. Bao, J. Deng, R. Zhai, D. Wang, X. Guo, Catal. Lett. 4 (1990) 25.
[16] X. Bao, G. Lehmpfuhl, G. Weinberg, R. Schlögl, G. Ertl, J. Chem. Soc., Faraday Trans. 88 (1992) 865.
[17] X. Bao, J.V. Barth, G. Lehmpfuhl, R. Schuster, Y. Uchida, R. Schlögl, G. Ertl, Surf. Sci. 284 (1993) 14.
[18] H. Schubert, U. Tegtmeyer, R. Schlögl, Catal. Lett. 28 (1994) 383.
[19] H. Schubert, U. Tegtmeyer, D. Herein, X. Bao, M. Muhler, R. Schlögl, Catal. Lett. 33 (1995) 305.
[20] W.S. Sim, P. Gardner, D.A. King, J. Phys. Chem. 99 (1995) 16002.
[21] X. Bao, J.F. Deng, D. Shuzhong, Surf. Sci. 163 (1985) 444.
[22] J. Deng, X. Xu, J. Wang, Y. Liao, B. Hong, Catal. Lett. 32 (1995) 159.
[23] J. Wang, X. Xu, J. Deng, Y. Liao, B. Hong, Appl. Surf. Sci. 120 (1997) 99.
[24] X. Bao, B. Pettinger, G. Ertl, R. Schlögl, Ber. Bunsenges. Phys. Chem. 97 (1993) 322.
[25] X. Bao, M. Muhler, B. Pettinger, Y. Uchida, G. Lehmpful, R. Schlögl, G. Ertl, Catal. Lett. 32 (1995) 171–183.
[26] X. Bao, M. Muhler, B. Pettinger, R. Schlögl, G. Ertl, Catal. Lett. 22 (1993) 215.
[27] X. Bao, M. Muhler, T. Schedel-Niedrig, R. Schlögl, Phys. Rev. B 54 (1996) 2249.
[28] T. Schedel-Niedrig, X. Bao, M. Muhler, R. Schlögl, Ber. Bunsenges. Phys. Chem. 101 (1997) 994.
[29] G.J. Millar, J.B. Metson, G.A. Bowmaker, R.P. Cooney, J. Chem. Soc., Faraday Trans. 91 (1995) 4149.
[30] G.J. Millar, M.L. Nelson, P.J.R. Uwins, Catal. Lett. 43 (1997) 97.
[31] G.J. Millar, M.L. Nelson, P.J.R. Uwins, J. Catal. 169 (1997) 143.
[32] C. Wang, G. Deo, I.E. Wachs, J. Phys. Chem. B 103 (1999) 5645.
[33] G.I.N. Waterhouse, G.A. Bowmaker, J.B. Metson, Appl. Surf. Sci. 214 (2003) 36.
[34] G.I.N. Waterhouse, G.A. Bowmaker, J.B. Metson, Appl. Catal. 265 (2004) 85.
[35] J.H. Je, T.S. Kang, D.Y. Noh, J. Appl. Phys. 81 (1997) 6716.
[36] N. Maréchal, E. Quesnel, Y. Pauleau, Thin Solid Films 241 (1994) 34.
[37] M. Riassian, D.L. Trimm, P.M. Williams, Chem. Soc. Lond.-Faraday Trans. I 72 (1976) 925.
[38] F. Tuinstra, J.L. Koening, J. Chem. Phys. 53 (1970) 1126.
[39] P. Lespade, A. Marchand, M. Couzi, F. Cruege, Carbon 22 (1984) 375.
[40] A.C. Ferrari, J. Robertson, Phys. Rev. B 61 (2000) 14095.
[41] D.Y. Zemlyanov, E. Savinova, A. Scheybal, K. Doblhofer, R. Schögl, Surf. Sci. 418 (1998) 441.